

## WELL PASSIVATING AND HIGHLY TEMPERATURE STABLE ALUMINUM OXIDE DEPOSITED BY ATMOSPHERIC PRESSURE CHEMICAL VAPOR DEPOSITION FOR PERC AND PERT SOLAR CELL CONCEPTS

Josh Engelhardt, Benjamin Gapp, Florian Mutter, Giso Hahn, Barbara Terheiden  
University of Konstanz, Department of Physics, 78457 Konstanz, Germany  
Josh.Engelhardt@uni-konstanz.de, Benjamin.Gapp@uni-konstanz.de, Florian.Mutter@uni-konstanz.de, Giso.Hahn@uni-konstanz.de, Barbara.Terheiden@uni-konstanz.de

**ABSTRACT:** Atmospheric pressure chemical vapor deposited aluminum oxide films based on trimethyl-aluminum and oxygen as precursors reaching a surface passivation quality comparable to atomic layer deposited aluminum oxide layers are presented. Demonstrated are charge carrier lifetime values up to 8 ms on n-type Cz-Si for fired  $\text{AlO}_x/\text{SiN}_x:\text{H}$  passivation stacks, common to PERC and PERT solar cell designs. The APCVD  $\text{AlO}_x$  layers are highly temperature stable for set peak firing temperatures in the range of 700-920°C allowing for surface recombination velocities  $< 2 \text{ cm}\cdot\text{s}^{-1}$ . The influence of temperature during  $\text{AlO}_x$  deposition in the APCVD tool is investigated concerning Si material and fundamental passivation effect properties. The latter are investigated in comparison to ALD  $\text{AlO}_x$  determining the underlying causes for higher lifetime after firing for APCVD  $\text{AlO}_x$  films.

**Keywords:** APCVD; aluminum oxide; passivation; PERC; PERT

### 1 INTRODUCTION

PERC (Passivated Emitter and Rear Cell) solar cells based on p-type crystalline Si and PERT (Passivated Emitter, Rear Totally diffused) solar cells based on n-type crystalline Si gain influence in the commercial solar cell market. Since the market is highly competitive, a low cost production is necessary. Such processes are feasible with high throughput, low cost and low upkeep production tools. Atmospheric pressure chemical vapor deposition (APCVD) tools fulfill these requirements and can supply the necessary layer quality for a high-efficiency solar cell production. Based on trimethyl-aluminum and  $\text{O}_2$  as precursors, aluminum oxide ( $\text{AlO}_x$ ) layers [01] are deposited, reaching a surface passivation quality comparable to atomic layer deposition (ALD) based  $\text{AlO}_x$  layers [02, 03]. APCVD  $\text{AlO}_x$  layers are deposited at higher temperatures, leading to a higher temperature stability during contact firing, *i.e.* preventing blistering effects in a set peak firing temperature range of 700 to 900°C. Application of APCVD  $\text{AlO}_x$  layers [04, 05] in PERC and PERT crystalline solar cell concepts is shown to be advantageous, while investigating the influence of the APCVD technology on current Si materials such as n-type Cz-Si for high-efficiency silicon solar cells.

High-efficiency solar cells often use monocrystalline n-type Si substrates due to the high bulk lifetime and lower susceptibility to degradation by impurities. However, n-type Si is prone to other degradation effects as oxygen-related defect formation having a negative impact on material quality. These defects develop during the different high temperature steps such as the APCVD process. A pre-high-temperature (pre-HT) step, sometimes referred to as 'tabula rasa' process, applied prior to any other solar cell process step helps to mitigate the oxygen-related defect formation [06-09]. Therefore, an investigation of temperature effects during APCVD deposition and possible solutions are investigated.

Subsequently, the passivation mechanisms of APCVD  $\text{AlO}_x$  are investigated in detail concerning the major factors affecting the passivation quality and in comparison to common ALD  $\text{AlO}_x$  layers. Special focus is laid on the temperature impact and influence during APCVD processing.

### 2 EXPERIMENTAL

n-type 2-4  $\Omega\text{cm}$  Cz- and 2-200  $\Omega\text{cm}$  FZ-Si wafers (156x156  $\text{mm}^2$  and 150 mm diameter, respectively) were wet chemically treated before a pre-HT step was performed on some of them. Following a second HF-dip to prepare the Si surface, APCVD (roller system, SierraTherm) or ALD (FlexAL, Oxford Instruments)  $\text{AlO}_x$  layers were deposited on both sides of the substrates before a possible annealing step in  $\text{N}_2$  atmosphere was performed. 40-90 nm PECVD (Plasma-Enhanced Chemical Vapor Deposition)  $\text{SiN}_x:\text{H}$  was subsequently deposited on some wafers to form the double layer passivation stack before firing in a belt furnace at a variety of set peak firing temperatures and charge carrier lifetime sampling by PCD (PhotoConductance Decay) and PL (PhotoLuminescence) techniques. References included samples with a stack of thermal  $\text{SiO}_x/\text{SiN}_x:\text{H}$  fired in a belt furnace. Molecular bond density, sputtering rate and elemental concentrations, refractive index and fixed charge density were measured by FTIR (Fourier Transform InfraRed spectroscopy), GD-OES (Glow Discharge Optical Emission Spectroscopy), ellipsometry and CV (Capacitance Voltage) technique on pure  $\text{AlO}_x$  coated FZ-Si samples, respectively.

### 3 RESULTS AND DISCUSSION

Inherent to the APCVD technique, a high temperature deposition is necessary to form the respective dielectric films by chemical reaction of precursor gases on the heated silicon substrate surface, as it is moved through the gas curtain (see Fig. 1). It affects bulk Si properties as well as film properties, *i.e.*,  $\text{AlO}_x$  layer passivation characteristics.

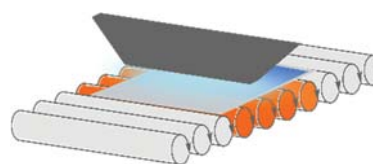


**Figure 1:** Schematic depiction of APCVD process.

### 3.1 Thermal impact from APCVD processing

The APCVD technique is based on the reactivity of precursor gases, *i.e.* trimethyl-aluminum (TMAI) and O<sub>2</sub> for AlO<sub>x</sub> layer deposition. In contrast to PECVD, the reaction energy is only provided by the surface temperature of the Si substrate heated, in this case by infrared light (set process temperature). The temperature can be used to influence and optimize the properties of the dielectric layers. Typical process set temperatures range from 400 to 800°C.

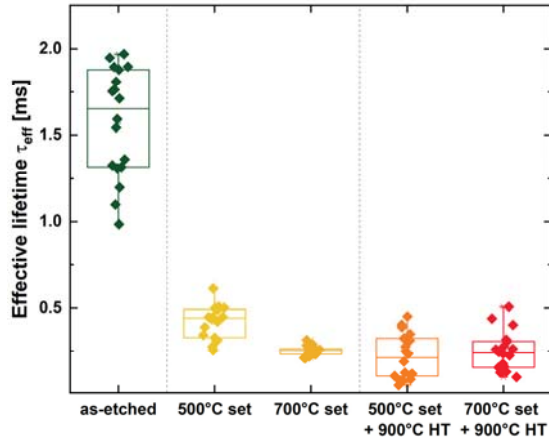


**Figure 2:** Box-plot diagram of effective lifetime  $\tau_{\text{eff}}$  for as-etched (green), solely temperature treated (yellow/ light orange) at 500°C and 700°C in APCVD (N<sub>2</sub> gas flow) or additionally after APCVD temperature treatment HT treated samples (dark orange/red). All samples are passivated by fired SiN<sub>x</sub>:H.

To investigate the effects of the heat treatment during AlO<sub>x</sub> deposition in an APCVD tool at typical temperatures, Cz-Si wafers were processed at 500 and 700°C for about 30-60 s without any process gases but N<sub>2</sub> to simulate duration and temperature budget of an AlO<sub>x</sub> deposition without the actual deposition of a film. A subsequent high temperature step (HT) at 900°C for about 10 min was carried out on some wafers of both groups. All wafers, including a non-temperature-treated group (as-etched), were passivated using fired SiN<sub>x</sub>:H. Fig. 2 shows the effective lifetime of all five groups, none of which had an initial pre-HT step before APCVD treatment. The drop in lifetime from 1.6 ms before temperature treatment in the APCVD reactor to below 500  $\mu$ s thereafter is dependent on the process temperature and cannot be reversed by a subsequent HT step at 900°C. Even SiN<sub>x</sub>:H with hydrogen passivation has evidently no impact on the bulk lifetime degradation.

PL images show circular patterns common to (new) thermal donors activated by temperature treatment below 800°C for a sufficiently long time. Literature indicates that a HT step before low temperature treatment mitigates or even prevents the formation of thermal donor clusters (ring structures *i.e.*, in n-type Cz-Si) and subsequent degradation of bulk lifetime [06-09].

As can be seen in Fig. 3, during processing in the APCVD tool pre-existing or forming crystal defects (ring structure in left image) are visible after passivation. A possible explanation could be decoration of defect sites with impurities. Samples undergoing a subsequent HT step at 900°C show a further degradation of the inner part of the ring (middle). Using a pre-HT step before all following

process steps prevents any occurrence of lifetime degrading effects (right).

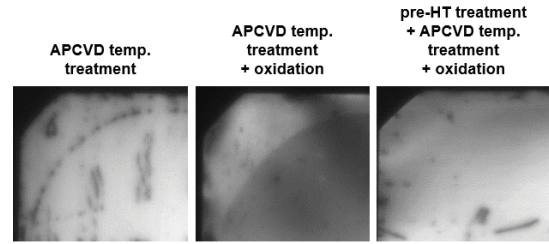


**Figure 3:** PL images of n-type Cz-Si wafers after APCVD heat treatment (left), APCVD heat treatment and HT step (middle), pre-HT step followed by APCVD heat treatment and HT step (right).

Since the pre-HT step has a significant influence for all further (H)T steps, the combination with a thermal oxidation was investigated. Some of the n-type Cz-Si wafers were pre-HT treated at 1000°C for 60 min before a low temperature treatment in the APCVD tool similar to the first experiment shown at around 500°C without deposition of AlO<sub>x</sub>. Subsequent HT treatment to grow a thermal SiO<sub>x</sub> at around 900°C in a tube furnace shows different effects on the effective lifetime for the four different groups in Fig. 4.

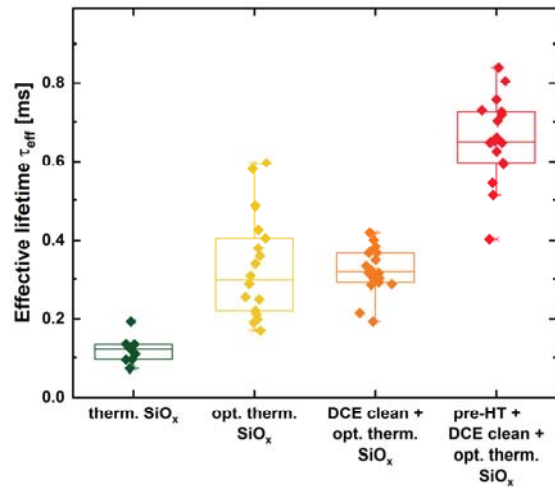


**Figure 4:** Effective lifetime of n-type Cz-Si wafers after low temperature treatment (APCVD) and subsequent passivation by fired thermal SiO<sub>x</sub>/SiN<sub>x</sub> stack. Shown are four different oxidation sequences with or without pre-HT step and/or DCE clean.

Passivation quality of thermal SiO<sub>x</sub> layer depends on growth parameters during oxidation and thermal history of the Si substrate. In this case, a standard oxidation step in a tube furnace leads to a low lifetime of around 100  $\mu$ s (green in Fig. 4) after subsequent SiN<sub>x</sub>:H deposition and firing step. By applying a DCE (1,2-dichlorethane) clean or a different set of thermal oxide growth parameters (orange and yellow in Fig. 4), the lifetime can be tripled. Yet the highest impact has an initial pre-HT step before APCVD treatment, leading to up to 800  $\mu$ s after thermal oxidation. Depending on n-type Cz-Si material quality and affinity to degradation, *i.e.*, thermal donor concentration, this effect of thermal donor activation prevention can vary.

The material shown here displayed a comparably strong thermal donor behavior.

### 3.2 Passivation for PERC and PERT solar cell concepts

APCVD  $\text{AlO}_x$  layer passivation quality highly depends on deposition parameters, *i.e.* deposition temperature, gas ratios, etc. as well as thickness (overall gas flow and/or belt speed dependent). Fig. 5 shows the effective lifetime  $\tau_{\text{eff}}$  of FZ-Si samples passivated by APCVD  $\text{AlO}_x$  of various deposition parameters. The passivation quality increases with layer thickness up to about 15 nm and remains stable for thicker  $\text{AlO}_x$  layers. Overall, an annealing step (HT step, *e.g.* firing) increases the charge carrier lifetime of samples from 12 nm up to an  $\text{AlO}_x$  layer thickness of about 25 nm, whereas at this thickness the lifetime decreases slightly for some APCVD process parameter sets. FZ-Si wafers with a base resistivity of 200  $\Omega\cdot\text{cm}$  show lifetimes up to 6.3 ms resulting in an effective surface recombination velocity of  $< 2 \text{ cm}\cdot\text{s}^{-1}$ . ALD  $\text{AlO}_x$  reference samples show a similar lifetime and surface recombination velocity level.

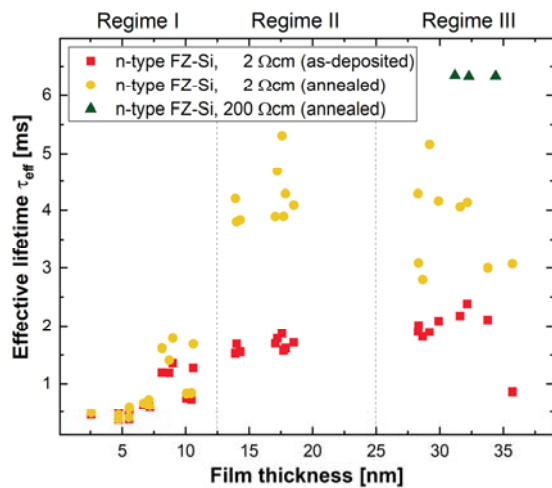


**Figure 5:** Effective lifetime  $\tau_{\text{eff}}$  of FZ-Si samples passivated by APCVD  $\text{AlO}_x$  of various deposition parameters dependent on the layer thickness. Samples are shown after deposition (red), after an HT annealing step (yellow) and with a 200  $\Omega\cdot\text{cm}$  base doping (green) for  $S_{\text{eff}}$  determination.

The overall level of up to 5 ms in effective lifetime and  $2 \text{ cm}\cdot\text{s}^{-1}$  in surface recombination velocity is a sufficiently high passivation quality for PERC as well as PERT rear sides with all the advantages of APCVD technology.

Further, APCVD  $\text{AlO}_x$  displays different interesting properties, *e.g.*, high firing temperature stability broadening the available parameter range for contact formation. In this case,  $\text{AlO}_x/\text{SiN}_x$  passivated n-type Cz-Si wafers are fired at 810-930°C set peak firing temperature. Four different optimized deposition parameter sets are used for  $\text{AlO}_x$  deposition in the APCVD reactor and two for ALD  $\text{AlO}_x$  (Fig. 6). All APCVD  $\text{AlO}_x$  layers reach lifetime values above 2 ms ( $T < 900^\circ\text{C}$ ) and up to 8 ms for a common PERC and PERT cell set peak firing temperature of 810°C. In comparison, samples passivated with either a single PECVD  $\text{SiN}_x:\text{H}$  layer or an optimized ALD  $\text{AlO}_x$  layer show only effective charge carrier lifetimes of below 3 and 5 ms after firing, respectively.

Therefore, optimized  $\text{AlO}_x$  layers from APCVD are

highly firing stable and allow for a firing parameter window between 700-900°C for PERC or PERT cell concepts. Furthermore, no blistering occurred during firing, allowing for homogeneous passivation without risking parasitic contact formation or loss in open circuit voltage,  $V_{\text{oc}}$ .

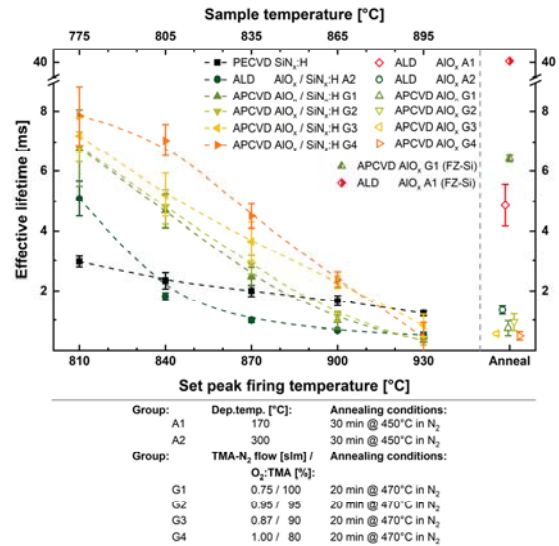


**Figure 6:** Effective lifetime  $\tau_{\text{eff}}$  of Cz- and FZ-Si samples passivated by APCVD and ALD  $\text{AlO}_x$  with various deposition parameters. In case of fired samples (left side of dashed vertical line),  $\text{SiN}_x:\text{H}$  coating was applied before. The annealed samples (details see below graph) are shown on the right side.

In case of annealed  $\text{AlO}_x$  films, ALD surpasses APCVD layers on Cz-Si by 5 to 1 ms and on FZ-Si by 40 to 6.5 ms, respectively. There seems to be a difference in passivation behavior and effectiveness depending on contact firing or annealing to activate the passivation ability.

### 3.3 Investigation into passivation effects

Obvious reasons for a difference in passivation depending on temperature treatment and coating layers are on the one hand H diff-/effusion [10] and blistering effects [11] due to the same H diffusion effect and on the other hand differences in the underlying primary or rather limiting passivation type (chemical or field effect passivation).

To investigate the differences between ALD and APCVD techniques in that regard, Cz- and FZ-Si samples of the various parameter groups from Fig. 6 were fabricated as pure  $\text{AlO}_x$  films on the Si substrates in an as-deposited or accordingly annealed state. The effective lifetime depicted in Fig. 7 (graph A) is similar to the previously in Fig. 6 obtained values. Important to mention is the fact that annealing does not increase the effective lifetime of APCVD films in the same way as it does in case of ALD  $\text{AlO}_x$  layers. The reason is the in-situ annealing of APCVD films during deposition and shortly afterwards in the cool-down section of the tool. A subsequent anneal does only marginally change the layers further with respect to molecular structure and thus diffusion of H or formation of fixed charges as is the case for ALD layers. The refractive index ranges around 1.6 as expected from literature [04] and shows no difference between ALD and APCVD (graph D). Subsequent GD-OES measurements on the other hand show a significant

difference in sputtering rate (graph B), indicating a lower film density for APCVD layers because of the higher sputtering rate. Thus, the  $\text{AlO}_x$  films are capable of better H diffusion allowing for less blistering in case of firing in a belt furnace with common  $\text{SiN}_x\text{:H}$  coating layers [05]. Furthermore, the GD-OES measurements show a slightly higher H concentration (atomic percentage) with a difference of up to 2.5%<sub>obs.</sub> in the APCVD  $\text{AlO}_x$  films compared to ALD (graph C). The Al/O ratio for APCVD is dependent on the total  $\text{O}_2$  flow during deposition as is the H content. While the latter decreases with  $\text{O}_2$  flow as expected considering the TMAI to be the H source during deposition, the Al/O ratio increases at the same time.

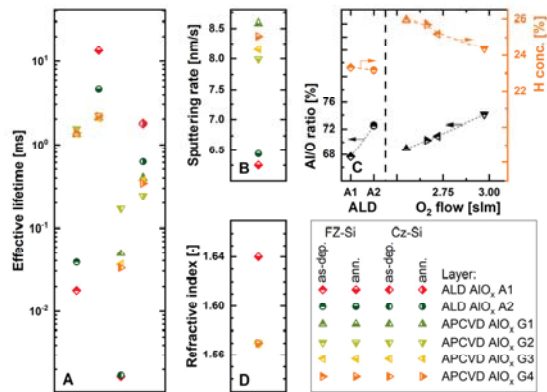


**Figure 7:** Effective lifetime  $\tau_{\text{eff}}$  of Cz- and FZ-Si samples passivated by APCVD and ALD  $\text{AlO}_x$  with various deposition parameters in as-deposited and annealed state (graph A). Corresponding refractive index and sputtering rate in graphs D and B, respectively. Graph C shows the Al/O ratio and H concentration of the layers.

An explanation can be found in molecular bond density that changes with  $\text{O}_2$  flow increasing the Al-O, Al- $\text{O}_2$  and Al- $\text{O}_4$  bonds in favor of Al- $\text{O}_6$  bonds to further an overall increase of incorporated Al in the APCVD  $\text{AlO}_x$  layer [15]. Fig. 8 shows the corresponding normalized molecular bond densities in the left graph and an example of an FTIR spectrum with identified bonds in the upper right graph.

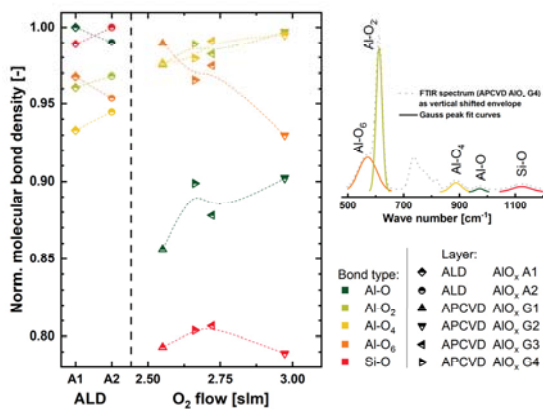


**Figure 8:** Normalized molecular bond density for all ALD and APCVD  $\text{AlO}_x$  layers (left graph) and example of an FTIR spectrum with identified bonds in the upper right graph.

A significant difference in bond density can be found for Si-O stemming from the interfacial silicon oxide layer between the  $\text{AlO}_x$  film and Si substrate. Previous publications indicate an importance of the growth and thickness of the interfacial  $\text{SiO}_x$  layer for chemical and field effect passivation quality [12, 13]. Since the relative bond density of Si-O is higher for ALD  $\text{AlO}_x$ , at least the chemical passivation properties of annealed ALD films are expected to be higher and explain the lack of the same in annealed APCVD layers. FTIR measurements further indicate the negative fixed charge density, known to depend on the density of Al on the surface of the interfacial  $\text{SiO}_x$  [12-14].

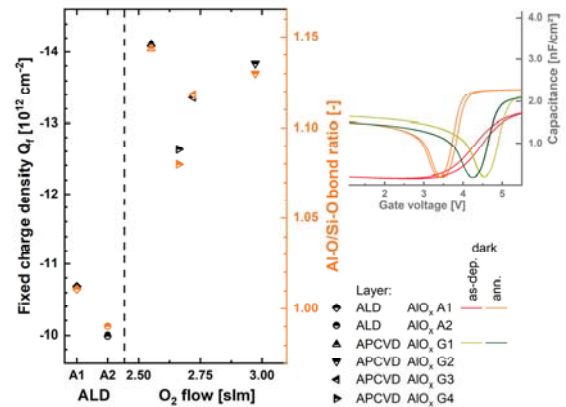


**Figure 9:** Negative fixed charge density from CV and Al-O/Si-O bond ratio from FTIR measurements (Fig. 8) for all ALD and APCVD  $\text{AlO}_x$  films. CV curves for dark measurements of one ALD and APCVD layer in as-deposited and annealed state in upper right graph.

CV measurements carried out with a Hg electrode setup show a 1.3 times higher negative fixed charge density in APCVD films compared to ALD  $\text{AlO}_x$  at a standard level of around  $1 \cdot 10^{13} \text{ cm}^{-2}$  (Fig. 9, left graph) [05]. Comparing the negative fixed charge density with the FTIR bond density, it turns out that the bond ratio of Al-O/Si-O is correlated with the negative fixed charge density, thus proving the aforementioned dependence on the Al density at the  $\text{SiO}_x$  interface. The CV curves in the upper right graph of Fig. 9 furthermore show the aforementioned change in the ALD layers during anneal (curve shape and slope changes from red to orange), while this does not occur in the in-situ annealed APCVD  $\text{AlO}_x$  films (CV curve does not change shape from light to dark green).

#### 4 CONCLUSION

$\text{AlO}_x$  layers by APCVD show high and stable passivation quality of up to 8 ms and above 2 ms even at high firing temperatures on n-type Cz-Si. With a surface recombination velocity of around  $2 \text{ cm} \cdot \text{s}^{-1}$  they are very well suited for PERC and PERT cell application with all the benefits of APCVD tool processing. The negative impact of the processing temperature during APCVD-deposition on n-type Cz-Si material quality can be reduced or even avoided by a pre-HT step or proper choice of material. A detailed characterisation investigating the passivation mechanisms of ALD and APCVD  $\text{AlO}_x$  films was presented to explain the differences between firing and lower temperature anneal on lifetime scale.

## 5 ACKNOWLEDGEMENTS

We would like to thank L. Mahlstaedt and B. Rettenmaier for their technical support. Part of this work was financially supported by the German Federal Ministry for Economic Affairs and Energy (FKZ 0324001 and 0324226A). The content is the responsibility of the authors.

## 6 REFERENCES

- [01] R. Hezel et al., *J. Electrochem. Soc.* **136**, No. 2, 518-523 (1989).
- [02] K.O. Davis et al., *Phys. Status Solidi RRL* **7**, No. 11, 942-945 (2013).
- [03] B. Semmache et al., *Proc. 29<sup>th</sup> EUPVSEC*, Amsterdam, Netherlands, 859-862 (2014).
- [04] L.E. Black et al., *Appl. Phys. Lett.* **100**, 202107 (2012).
- [05] L.E. Black et al., *Sol. Energ. Mat. Sol. Cells* **120**, 339-345 (2014).
- [06] V. LaSalvia et al., *Proc. 43<sup>rd</sup> IEEE PVSC*, Portland, Oregon, USA, 1047-1050 (2016).
- [07] R. Falster et al., *Solid state phenomena* **57-58**, 123-128 (1997).
- [08] D. C. Walter et al., *Proc. 28<sup>th</sup> EUPVSEC*, Paris, France, 699-702 (2013).
- [09] E. E. Looney et al., *Appl. Phys. Lett.* **111**, 132102 (2017).
- [10] A. Richter et al., *IEEE J. Photovol.* **3**, No. 1, 236-245 (2013).
- [11] T. Lüder et al., *En. Proc.* **27**, 426-431 (2012).
- [12] G. Dingemans et al., *J. Appl. Phys.* **110**, 093715 (2011).
- [13] Y. Zhao et al., *Nanoscale Res. Lett.* **8**:114 (2013).
- [14] V. Naumann et al., *En. Proc.* **27**, 312-318 (2012).
- [15] J.M. Reyes et al., *J. Electrochem. Soc.* **160**, No. 10, B201-B206 (2013).